On Co-Existence of In-Band UWB-OFDM and GPS Signals: Tracking Performance Analysis

Dmitriy Garmatyuk, *Member, IEEE*, Y. Jade Morton, *Member, IEEE*, and Xiaolei Mao
Department of Electrical and Computer Engineering
Miami University, Oxford, OH 45056 USA

***Abstract*— The problem of in-band co-existence between GPS and other potential interfering signals is viewed from the following angle in this paper: Is there a coding or modulation technique which would permit simultaneous use of GPS and other RF services occupying same bandwidth? Very low interference between the UWB radar and GPS signals can be achieved by shaping radar pulses using orthogonal frequency division multiplexing (OFDM) coding, which is a multi-carrier modulation technique targeted for commercial UWB communications. The paper shows that we can, in fact, expect a very good degree of interoperability of a system used for GPS reception and UWB-OFDM radar purposes. The benefits of using UWB sensor in conjunction with GPS can be for example, to supplement positioning algorithms with radar-collected data, as well as to perform general reconnaissance of the surrounding area. The paper includes detailed analysis of the proposed multiple-use UWB-OFDM radar/GPS receiver concept, the effect of co-existing UWB-OFDM signals on GPS receiver tracking loop carrier noise level, and the impact on the quality of GPS solution in weak GPS signal environment. A brief discussion of MATLAB implementation of the modeled scenarios is presented as well.**

***Index Terms*—OFDM, GPS, coexistence**

I. Introduction

Airborne reconnaissance, surveillance and navigation operations benefit considerably from using radar imagery of the underlying terrain and objects embedded in it. Desired resolution of images is attained via configuring the system as synthetic aperture radar (SAR) and subsequent processing of received SAR signals known as focusing [1]. As aircraft mission and goals are growing in importance and sophistication, the demands on on-board radar systems are also increasing. The devices are becoming more complex, yet the desire to conserve payload space and weight in airborne platforms remains. This has led to research of systems with multiple uses – e.g. radar and communications [2].

Relatively recent advent of unmanned aerial vehicles (UAV) into battlefield operations also has brought about new challenges and opportunities. Particularly, in light of increasing importance of military operations in urban terrain (MOUT) the gap between short-range and long-range radar imaging scenarios appears to narrow, as target ranges may be as short as less than 100 meters. Numerous sensor design challenges abound in these cases, with the following three areas, among others, being of interest to imaging radar designers:

- Power/weight/cost: All three must be minimized to ensure longer operation time and deployment affordability on multiple platforms;
- High resolution of imagery: Many targets in MOUT scenarios are inherently relatively small-size – makeshift redoubts, overturned cars, piles of rubble, etc;
- Communication capabilities and resistance to interference from friendly platforms, or jamming from hostile systems.

These challenges are currently being addressed by many research teams which led to the concept of mini-SAR [3, 4]. The concept of miniaturized, potentially multiple-use, high-resolution all-weather imaging and navigation sensor can be addressed from several different perspectives; the purpose of this paper is to suggest the solution via utilizing UWB orthogonal frequency division multiplexing (OFDM) system architecture, which will also allow simultaneous reception and analysis of GPS signals, thus obviating the need to have a separate receiver antenna and front-end for GPS. Most types of UWB waveforms share a feature which may be considered a disadvantage in certain scenarios: their instantaneous spectrum is pre-determined by the radar system design and cannot be adjusted during operation. Hence a low opportunity for co-existence between these types of UWB signals and received GPS waveforms [5], which may lead to the increased chance of GPS performance interrupts, or to the need to put elaborate isolation schemes and protocols in place, particularly if same-platform functionality of UWB and GPS systems is desired. OFDM, as a fully-digital, multi-frequency modulation technique, can overcome this problem via simple pulse construction procedure. OFDM signal spectrum can be adjusted on a pulse-to-pulse basis, thus allowing for high potential for co-existence between it and any narrowband system functioning on the same platform. The two systems then can be used separately, or complement each other in various types of environments.

OFDM as a method of digital modulation is not a new technique – its concept was explored in 1960's by several researchers, e.g. [6]. However, it was not until the beginning of the 2000's that this technique and corresponding system

architecture started being considered for wideband applications. There were two major reasons precluding UWB implementation of OFDM: Federal Communications Commission's (FCC) ban on commercial use of wide swaths of spectrum, which was lifted for extremely low-power signals in 2002; and unavailability of fast, inexpensive analog-to-digital (A/D) and digital-to-analog (D/A) converters [7], as they are significant components of an OFDM system determining its bandwidth. As soon as these two hurdles were overcome, UWB OFDM became a focus of R&D efforts in the industry and academia with an emphasis on commercial broadband communications [8–10].

Despite several significant advantages UWB-OFDM system architecture was not previously considered for applications in high-resolution radar. This paper will introduce the model of such a system and it will also demonstrate the high potential for in-band co-existence of OFDM waveforms with GPS signals. The analysis will then extend to performance simulation of GPS signal recovery and tracking using UWB-OFDM radar receiver model.

II. UWB-OFDM System Model

As any UWB system, UWB-OFDM architecture can be used to produce high-resolution images via SAR data collection and processing [11]. It also possesses a viable quality of being able to perform as a high data rate communication system, which makes it a good candidate for multiple use implementations. In this paper we will focus on another aspect of OFDM signaling – ability to co-exist with narrowband signals and interferers. We start with OFDM signal construction and system modeling, which will be discussed in this section.

A. OFDM Signal Design

The time-domain form of a baseband OFDM signal is given by:

$$s_{OFDM}(t) = \sum_{k=1}^{N} x_k \exp\left[j2\pi k \frac{t}{T} \right], \quad 0 < t < T \tag{1}$$

where x_k is a set of coefficients which determine the amplitude and/or phase of an individual sub-band of the signal and T is the total pulse duration, which is tied to the total number of sub-bands N and also to the sampling rate of OFDM transmitter's D/A converter. However, it is more intuitive to begin OFDM signal design in the frequency domain – as these waveforms are multi-frequency constructions resulting from summation of orthogonal RF pulses. Equation (2) shows a discrete-value vector $\mathbf{S}_{OFDM}$ representing spectral components to be translated into OFDM signal with zero DC-component:

$$\mathbf{S}_{OFDM} = [x_N \; x_{N-1} \; \ldots \; x_1 \; 0 \; x_1 \; x_2 \; \ldots \; x_N], \text{ where } x_k = \{0; \pm 1\} \tag{2}$$

Notation {…} describes the set of possible vector component values. The resultant vector $\mathbf{S}_{OFDM}$ is discrete mathematical spectrum of the OFDM signal in conventional notation. The subsequent operation performed on $\mathbf{S}_{OFDM}$ is inverse Fourier transform, which can be implemented as IFFT using a microprocessor designed for this goal, or in software, depending on the desired speed of application. The conversion from the digital format of the signal to analog baseband form is performed via D/A conversion. As can be easily seen, the number of samples output by the D/A converter is equal to the number of samples originally defined in vector $\mathbf{S}_{OFDM}$ – thus, the total duration of an OFDM pulse is $T = (2N - 1)\,\Delta t = (2N - 1)/F_s$, where Δt is the sampling interval of the D/A converter and F_s is its sampling frequency. Further analysis of the resultant waveform in frequency domain reveals that the spectrum of OFDM signal is a collection of equally spaced *sinc*-functions with weights x_k as shown in Fig. 1. This result is fundamental to our subsequent model of a dual-use radar/GPS system, as it clearly implies the easy procedure of forming OFDM radar pulses with nulling of the sub-bands which may potentially interfere with GPS signals.

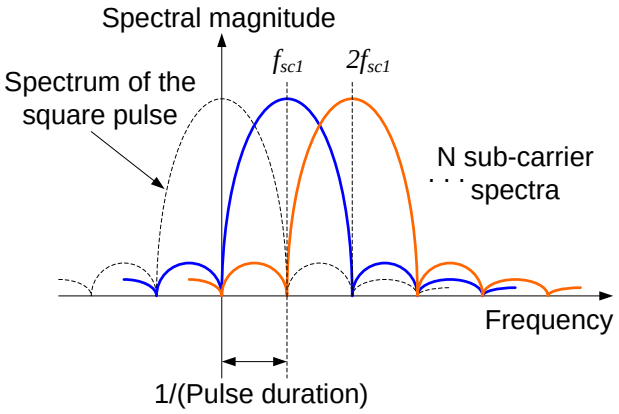

Fig. 1 Conceptual representation of an OFDM signal spectrum use

We can then show that, given the number of sub-bands N and D/A converter sampling frequency F_s, we can find the indices k of vector $\mathbf{x} = [x_1 \; x_2 \; \ldots \; x_N]$ which are to be nulled as:

$$k_n = ROUND\left(\left[\frac{N\left| f_0^{GPS} - f_0^{OFDM} \right| - \Delta f^{GPS}}{F_s} \; \ldots \; \frac{N\left| f_0^{GPS} - f_0^{OFDM} \right| + \Delta f^{GPS}}{F_s} \right] \right), \tag{3}$$

where f_0^{GPS} and Δf^{GPS} are center frequency and bandwidth of a GPS signal, respectively, and f_0^{OFDM} is the carrier frequency of UWB-OFDM signal. This represents minimum requirement and more sub-bands may be nulled to achieve better performance.

B. UWB-OFDM Signal Model: Numerical Example

For our simulation study we chose the sampling frequency of a D/A converter in OFDM transmitter to be 1 Gs/s – which is quite realistic for present-day commercial off-the-shelf (COTS) component base. We also chose the number of sub-bands N = 32, which would result in a 64 ns pulse duration. Furthermore, we dropped the value of (–1) from the x_k alphabet, therefore the baseband OFDM signal discrete sample representation in time domain becomes:

$$s_{OFDM}(t_n) = \Pi(64ns)\sum_{k=1}^{32} x_k \cdot \cos\left(2\pi k f_{sc1} t_n\right), \quad (4)$$

where $\Pi(64ns)$ is a square pulse of 64 ns duration and fsc1 is the frequency of first sub-carrier (center of sub-band), which is calculated as the inverse of the total length of the OFDM pulse – 64 ns in our case, thus f_{sc1} = 15.625 MHz. To calculate total bandwidth of the resultant baseband pulse we simply multiply f_{sc1} by the number of sub-bands, i.e. – 15.625 MHz multiplied by 32, or 0.5 GHz. This is consistent with the expected bandwidth figure derived from sampling rate of 1 Gs/s.

Further construction of an UWB-OFDM simulated radar signal included building a pulse train with varying pulse shapes. Each 65-sample pulse was followed by 935-sample zero sequence inserted to simulate down-time processing interval – roughly translated to 100 meter range of the imaging radar. These 1000-sample segments were assembled into a 10-pulse train as shown in Fig. 2.

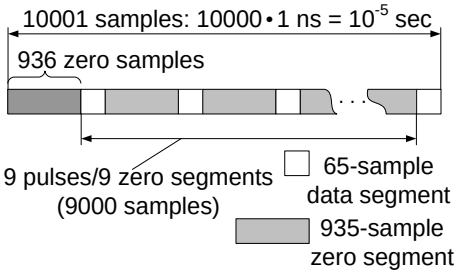

Fig. 2 UWB-OFDM radar pulse train diagram

C. Dual-Use Receiver Model

Since the goal of our study is to test the performance of simultaneous in-band reception of GPS signals via UWB-OFDM radar receiver, we defined the receiver model as shown in Fig. 3. In it, the receiver signal $s_{rx}(t)$ is a sum of UWB-OFDM and GPS signals, and AWGN $n(t)$. This signal was modeled as a 20 Gs/s waveform to approximate realistic analog form. The carrier frequency of UWB-OFDM signal is set to 1.8GHz and the GPS signal is chosen be an L1 band civilian GPS with 1.57542 GHz carrier frequency.

Bandpass filter was chosen to be an elliptic filter implemented in MATLAB with the following parameters: center frequency = 1.57542 GHz, transition band = 10 MHz, maximum ripple magnitude in passband 0.1 dB and maximum ripple magnitude in stopband –60 dB. This yielded a filter of 6th order.

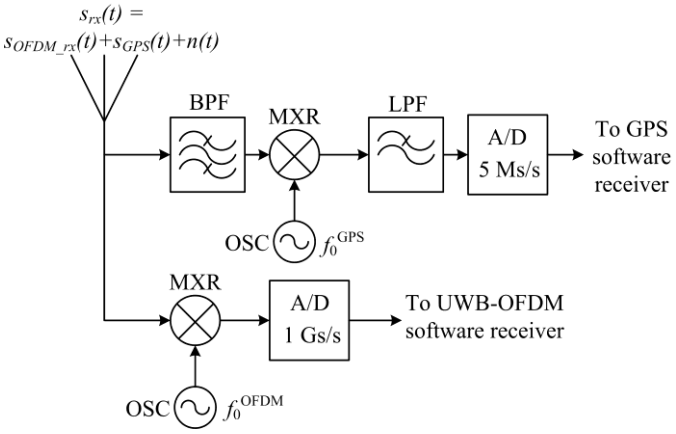

Fig. 3 Block diagram of dual-use OFDM/GPS receiver front end model (without amplifiers)

Next section will describe construction and implementation of GPS software receiver used in subsequent simulation study.

III. GPS Software Receiver

A software GPS receiver works with direct sampled RF signals or IF signals containing the GPS bands. In this project, the A/D outputs shown at Fig. 3 are used as inputs to the software receiver to perform GPS signal acquisition, tracking, navigation data decoding, bit synchronization, and ultimately, navigation processing. In our previous studies, we presented the GPS signal acquisition performance [12]. The acquisition process provides coarse estimation of a GPS signal's Doppler frequency and code phase. This coarse estimation will be used to initialize the code and carrier tracking loops to obtain refined code and carrier phase, Doppler frequencies, and navigation bit transitions edge. In this paper, we will focus on signal tracking performances.

A high level GPS signal tracking loop is shown in Fig. 4. A GPS tracking loop contains a carrier tracking loop and a code tracking loop. The digitized input data contains multiple baseband GPS signal and receiver noise samples. At the initial stage of the tracking, the coarse Doppler frequency and code phase of a satellite obtained from the acquisition process are used to initialize the tracking. Once the tracking loop is in lock, the code tracking loop provides a so-called prompt code whose code phase is driven to align with that of the incoming signal, while the carrier tracking loop outputs the carrier Doppler and carrier phase (if the carrier tracking loop is implemented as a phase lock loop) or carrier Doppler frequency only (if the carrier tracking loop is implemented as a frequency lock loop). The code phase, carrier Doppler and carrier phase are then fed back to the correlators to perform code and carrier wipe off for the next block of data.

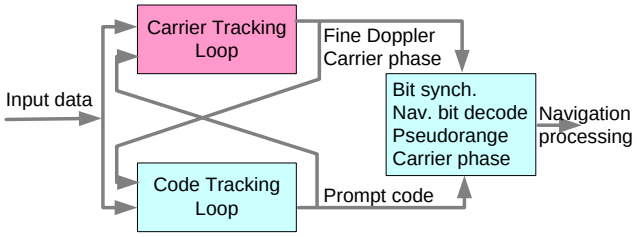

Fig. 4. A high level block diagram of the GPS signal tracking loop

The carrier tracking loop is the weak link in the entire tracking process. The performance of the carrier tracking loop is a good indicator of the GPS receiver's performance. Fig. 5 shows a more detailed block diagram of the carrier tracking loop.

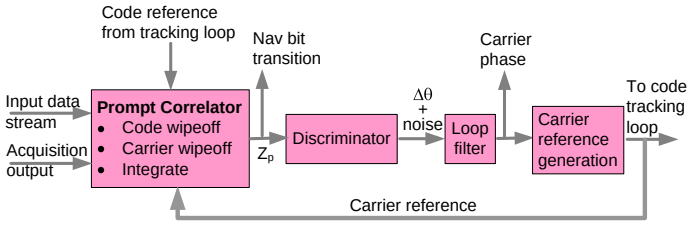

Fig.5. Block diagram of a carrier phase tracking loop

The first component of a carrier tracking loop is a correlator that wipes off the code and carrier from the input and then integrates the resultant signal. This is the same correlator as the prompt correlator in the code tracking loop. With a software receiver, the real digitized input stream from Fig. 3 can be immediately down-converted to a complex baseband signal:

$$s_{GPS}(t) = aC_a(t-\tau)D(t)e^{j(\omega_d t+\theta_0)} + \varepsilon \qquad (5)$$

where, a, C_a, τ, D, ω_d, and θ_0 are the amplitude, CA code, CA code phase, Navigation data bit value, Doppler frequency, and initial carrier phase of a satellite signal, respectively. The receiver noise, all remaining satellite signals, and UWB leakage from neighboring sub-bands are lumped into ε. If the code reference generated by the code tracking loop is $C_a(t-\hat{\tau})$, and the carrier Doppler and phase generated by the carrier phase loop output are $\hat{\omega}_d$ and $\hat{\theta}_0$, respectively, the correlator output is:

$$\begin{aligned} z_p &= \int_{T_I} s_{GPS}(t)C_a(t-\hat{\tau})e^{-j(\hat{\omega}_d t+\hat{\theta}_0)}dt \\ &= a\int_{T_I} D(t)C_a(t-\tau)C_a(t-\hat{\tau})e^{j\left[\Delta\omega_d t+\Delta\theta_0\right]}dt + \varepsilon_{Zp} \end{aligned} \qquad (6)$$

When the code delay lock loop is in lock and if the integration does not occur across a navigation data bit transition, then

$$z_p = aD\sin c\left(\frac{\Delta\omega_d T_I}{2}\right)e^{j\left[\frac{\Delta\omega_d T_I}{2}+\Delta\theta_0\right]} + \varepsilon_{Zp} \qquad (7)$$

When the carrier tracking loop is locked,

$$z_p \approx aD + \varepsilon_{Zp} \qquad (8)$$

The navigation data bit transition can be extracted from the prompt correlator output.

The correlator output is used as the input to a discriminator to generate a measure of the carrier phase error between that of the input signal and the carrier tracking loop output. The existence of the navigation data bit introduces phase ambiguities to the tracking loop. Costas discriminators can tolerate the navigation data bit sign. We used the following Costas discriminator in our carrier tracking loop:

$$\Theta = \tan^{-1}\frac{\mathrm{Im}(Z_p)}{\mathrm{Re}(Z_p)} \qquad (9)$$

Substituting (7) into (9), we get $\Theta = \Delta\theta$ for $\Delta\theta < \left|\frac{\pi}{2}\right|$, if there is no noise in the correlator output.

To reduce the presence of noise, a loop filter is needed to smooth the discriminator output. Carrier phase measurement is extracted from the output of the loop filter. A loop filter order determines the dynamic response performance of the carrier tracking loop. A second order loop filter is sufficient to track a low dynamic platform. In order to track platform accelerations, a third order loop filter is needed. In the presence of strong leakage from other UWB sub-bands when the UWB power is high, additional signal processing needs to be incorporated into the tracking loop to maintain lock. With the software receiver architecture, batch-based processing can be used to enhance GPS signal observability and provide improved performance under reduced GPS signal to noise ratio conditions. For example, regression can be applied to a sequence of raw carrier phases obtained at the discriminator output to reduce the carrier phase noise and provide tighter feedbacks to tracking loop input for carrier wipe off. The order of the regression function can be adjusted to fit the dynamic condition of the radar platform [13]. Other on-board sensors such as inertial navigation sensor can also provide platform dynamic correction information to the receiver to reduce the tracking loop performance threshold [14]. In this paper, however, we will evaluate the UWB-GPS dual use platform under the hypothesis that the receiver is stand-alone mode and that only conventional tracking procedure will be used in the performance evaluations.

IV. Performance Analysis and Results

A. Joint UWB-OFDM and GPS Signal Model

As discussed in Section II we aim to create a model of a received signal expressed as:

$$s_{rx}(t) = s_{OFDM\_rx}(t) + s_{GPS}(t) + n(t)\ , \qquad (10)$$

and this signal is generated at 20 Gs/s sample rate to

approximate analog behavior. Both GPS and UWB-OFDM signals were generated by up-converting their baseband versions to respective carrier frequencies. The baseband signal representations are also used to calculate the signal-to-signal ratio (SSR), as shown:

$$SSR = 10\log_{10}\left(\frac{\left\langle s_{GPS\_BB}(t_{PT}), s_{GPS\_BB}(t_{PT})\right\rangle}{\left\langle s_{OFDM\_BB}(t_{PT}), s_{OFDM\_BB}(t_{PT})\right\rangle}\right) \quad (11)$$

where t_{PT} refers to time vector of pulse train samples shown in Fig. 2 and s_{GPS_BB} and s_{OFDM_BB} represent baseband GPS signal and baseband OFDM pulse train, both of 10 μs of total duration and both sampled at 1 Gs/s. In OFDM signal all 32 sub-band coefficients are assigned randomly on a pulse-to pulse basis, except sub-bands 13 through 16, which were nulled for all generated pulses to reduce interference with GPS signals. An illustration of the resultant spectra of baseband GPS signal segment and OFDM pulse train for $SSR \approx -40$ dB is shown in Fig. 6.

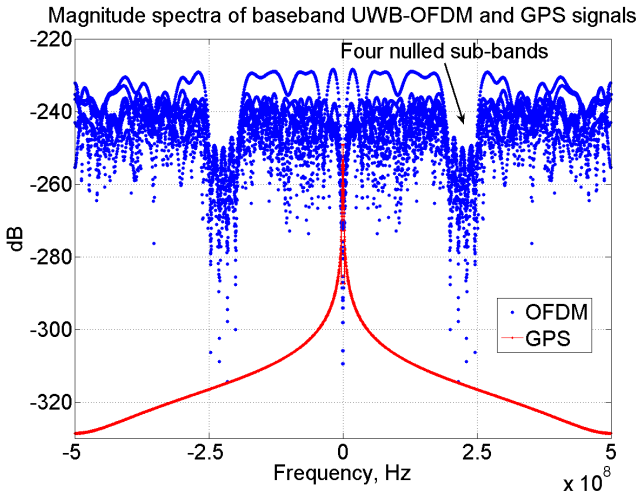

Fig. 6 Magnitude spectra of 10 μs segments of baseband GPS and OFDM train pulse at $SSR \approx -40$ dB

B. Simulation Results

Our first test case involved the recovery of a GPS signal under various SSR conditions. Several 10 μs $s_{rx}(t)$ signal segments were generated and the recovered GPS signal from s_{rx} was contrasted with the original GPS signal copy to produce the error estimate –

$$Error = \sqrt{\frac{1}{N_s}\sum_{k=1}^{N_w}\left(s_{GPS} - \hat{s}_{GPS}\right)^2} \quad (12)$$

where N_s is a total number of samples of GPS signal in a 10 μs interval and $\hat{s}_{GPS}$ is a GPS signal recovered from the received signal after bandpass filtering. Illustration of the results is shown in Fig. 7.

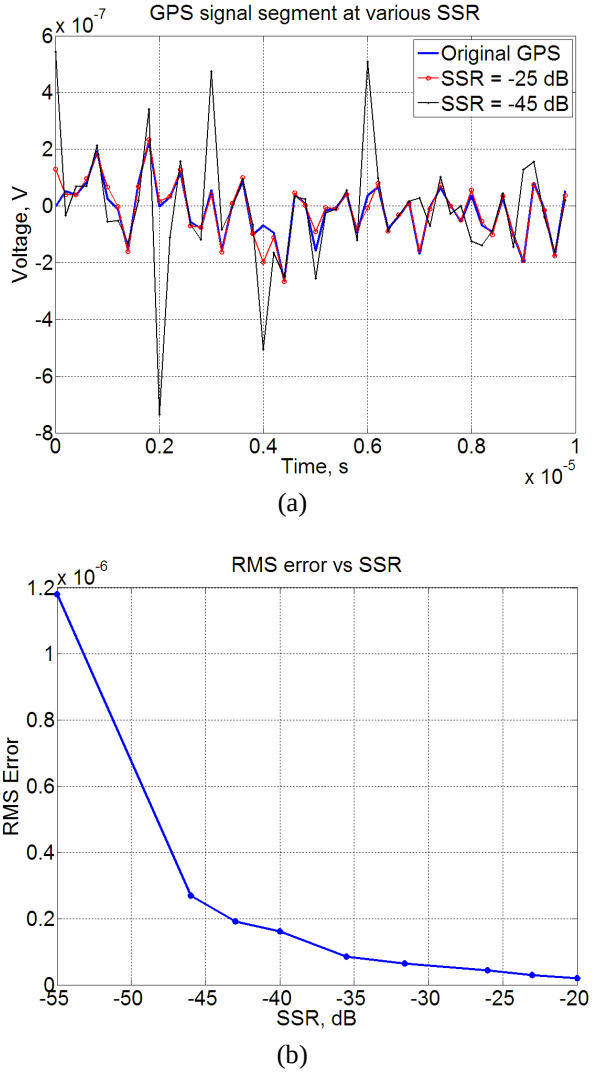

Fig. 7 GPS signal recovery at various SSR: (a) – Time domain example; (b) – RMS error calculated for 10 μs segment.

C. Tracking Performance

The tracking performance is evaluated for input civil GPS signals located at the L1 band with 46 dB-Hz carrier to noise ratio. The correlations were performed using 1ms data blocks. A Costas discriminator shown in Equation (8) is applied to the correlator output. A second order loop filter is implemented to reduce the noise contribution to carrier phase estimation at the discriminator output. Due to the high sampling rate used to generate the input data, a large computational time is required to generate adequate amount

of UWB and GPS signals. As a result, we limit our evaluations to tracking 50ms of data. Fig. 8 shows example discriminator outputs for two sequences of input data: one with only GPS signals and noise in the input, the other with added UWB signals. The GPS to UWB signal to signal ratio is -40 dB across the entire UWB band. Note the higher variations of the carrier phase error for the combined UWB and GPS signal sequence.

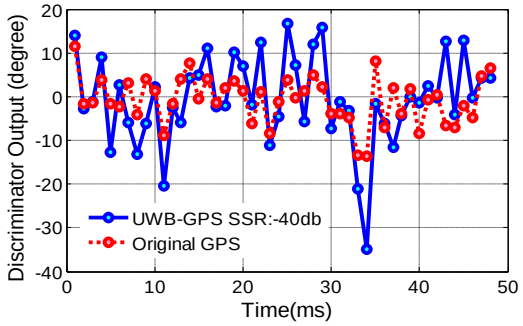

Fig. 8. Raw carrier phase errors generated by the software GPS receiver carrier tracking loop discriminator. Two data sequences are shown in the figure: one contains only GPS and noise, the other contains the same GPS sequence and noise but a UWB signal is superimposed on it.

We performed tracking performance evaluations for sequences with SSB ranging from -45dB to -20dB. Each sequence data length is 50ms. We computed the standard deviation of the carrier phase error for each of the sequence. Fig. 9 plots the carrier phase error standard deviation as a function of the GPS to UWB signal to signal ratio. Note that the original GPS signal with nominal signal power level maintains carrier phase tracking error at about 6 degrees. When co-existing with UWB signals, if the SSR is above -25 dB, the leakage from neighboring UWB sub-bands has very small impact on the carrier phase tracking loop performance. The impact becomes more noticeable at SSR=-35 dB where there is about 1 degree of increase in the carrier phase error standard deviation. At SSR=-45 dB, the carrier phase error is about 11 degrees, nearly double the amount when UWB is absent. At SSR=-50 dB, the carrier tracking loop loses lock.

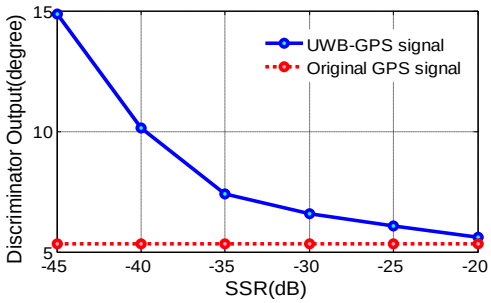

Fig. 9. GPS receiver carrier tracking error standard deviation as a function of GPS to UWB SSR.

V. Conclusions

The problem of in-band co-existence between GPS and other potential interfering signals can also be viewed from a different angle: Is there a coding or modulation technique which would permit simultaneous use of GPS and other RF services occupying same bandwidth? The benefits of using UWB sensor in conjunction with GPS can be for example, to supplement positioning algorithms with radar-collected data, as well as to perform general reconnaissance of the surrounding area. When assembled in a wireless sensor network, UWB systems present even more advantages for positioning and navigation operation. Very low interference between the UWB and GPS signals can be achieved by shaping radar pulses using orthogonal frequency division multiplexing (OFDM) coding, which is a multi-carrier modulation technique targeted for commercial UWB communications. Recent technological innovations can make UWB-OFDM applications feasible and relatively inexpensive. In particular, advent of 1 Gs/s (and above) sampling technology in mass-produced standalone chip component base has facilitated the implementation of OFDM on UWB scale in commercial communications technology, opening up the possibilities of using the same architecture for both radar and data transfer purposes. UWB-OFDM sensor will possess the same advantages as other wideband systems and will add more benefits in many usage scenarios. Dynamic spectrum allocation achieved by digital signal processing in OFDM bodes extremely well for minimizing interference between it and narrowband signals, such as GPS, as opposed to the majority of other UWB signals whose instantaneous spectrum is pre-determined by the radar system design and cannot be adjusted during operation.

A software GPS receiver is an ideal platform to be integrated with the UWB radar to obtain the position solutions. Our previous study confirmed the potential for co-existence by generating separate UWB-OFDM and GPS signals and simulating a cumulative signal containing their sum by placing nulls in UWB-OFDM signal spectrum coincided with the expected location of GPS signal band. In this paper, four OFDM sub-carriers were turned off at the vicinity of the GPS band. The GPS signal band was recovered by bandpass filtering. Batch processing is implemented to track the GPS carrier. The processing used 1ms integration time, a conventional Costas discriminator, and second order loop filter. For nominal GPS input signal with carrier to noise ratio at 46 dB-Hz, this conventional tracking loop can generate carrier phase errors with standard deviation of about 6 degrees. When co-existing with UWB signals, the carrier phase error increases as the GPS to UWB signal to signal ratio decreases. For SSR above -25 dB, there is very little impact on the GPS carrier tracking loop performance. At SSR=-45 dB, the carrier phase error standard deviation nearly doubles the level at which where there is no UWB signals. The conventional carrier tracking loop loses lock when SSR is -50 dB. More robust tracking loop can be implemented to allow the GPS receiver to have lower carrier phase error and to reduce the threshold at which the receiver loses lock.

ACKNOWLEDGMENT

This work is supported by the U.S. Air Force Office of Scientific Research under Grant FA9550-07-1-0297.

REFERENCES

[1] M. Soumekh, "Reconnaissance with ultra wideband UHF synthetic aperture radar," *IEEE Signal Processing Mag.*, vol. 12, no. 4, pp. 21–40, Jul. 1995.

[2] G. N. Saddik, R. S. Singh, and E. R. Brown, "Ultra-wideband multifunctional communications/radar system," *IEEE Trans. Microwave Theory Techn.* , vol. 55, no. 7, pp. 1431–1437, Jul. 2007.

[3] *Sandia MiniSAR – Miniaturized Synthetic Aperture Radar*, Sandia National Laboratories, Albuquerque, NM. Available: http://www.sandia.gov/RADAR/minisar.html

[4] M. Edrich, "Ultra-lightweight synthetic aperture radar based on a 35 GHz FMCW sensor concept and online raw data transmission," in *IEE Proc. Radar, Sonar Navig.*, vol. 153, pp. 129–134, Apr. 2006.

[5] M. Hämäläinen, V. Hovinen, R. Tesi, J. H. J. Iinatti, and M. Latva-aho, "On the UWB system coexistence with GSM900, UMTS/WCDMA and GPS," *IEEE Journ. Sel. Areas Communications*, vol. 20, no. 9, pp. 1712–1721, Dec. 2002.

[6] R. Chang and R. Gibby, "A theoretical study of performance of an orthogonal multiplexing data transmission scheme," *IEEE Trans. Communications*, vol. 16, no. 4, pp. 529–540, Aug. 1968.

[7] Bin Le, T. W. Rondeau, J. H. Reed, and C. W. Bostian, "Analog-to-digital converters," *IEEE Signal Processing Mag.*, vol. 22, no. 6, pp. 69–77, Nov. 2005.

[8] *TI Physical Layer Proposal: Time-Frequency Interleaved OFDM*, Texas Instruments, Dallas, TX, 2003. Available: http://focus.ti.com/lit/an/slla138/slla138.pdf

[9] A. Batra, J. Balakrishnan, G. R. Aiello, J. R. Foerster, and A. Dabak, "Design of a multiband OFDM system for realistic UWB channel environments," *IEEE Trans. Microwave Theory and Tech.*, vol. 52, no. 9, Part 1, pp. 2123–2138, Sep. 2004.

[10] C. Snow, L. Lampe, and R. Schober, "Performance analysis of multiband OFDM for UWB communication," in *Proc. 2005 IEEE Int. Conf. Communications*, Seoul, Korea, 2005, vol. 4, pp. 2573–2578.

[11] D. Garmatyuk, "Simulated imaging performance of UWB SAR based on OFDM," in *Proc. 2006 IEEE Int. Conf. Ultra-Wideband*, Waltham, MA, pp. 237–242, Sept. 2006.

[12] D. Garmatyuk and Y.T. Morton, "On coexistence of in-band UWB-OFDM and GPS signals," Proc. *2007 The Institute of Navigation National Technical Meeting*, San Diego, CA, Jan. 22-24, 2007.

[13] X. Mao, Y. T. Morton, and Q. Zhou, "Regression-based algorithm for weak GPS signal carrier tracking on dynamic platform," to be submitted.

[14] Soloviev, A., Gunawardena, S., van Graas, F., "Deeply integrated GPS/low cost IMU for low CNR signal processing: flight test results and real time implementation," Proc. 2004 Institute of Navigation Global Navigation Satellite Systems Conference, pp. 1621-1631, Long Beach, CA, Sept. 2004.